Hidden Poison: Machine Unlearning Enables Camouflaged Poisoning Attacks

Anonymous authors
Paper under double-blind review

Abstract

We introduce *camouflaged data poisoning attacks*, a new attack vector that arises in the context of machine unlearning and other settings when model retraining may be induced. An adversary first adds a few carefully crafted points to the training dataset such that the impact on the model's predictions is minimal. The adversary subsequently triggers a request to remove a subset of the introduced points at which point the attack is unleashed and the model's predictions are negatively affected. In particular, we consider clean-label *targeted* attacks (in which the goal is to cause the model to misclassify a specific test point) on datasets including CIFAR-10, Imagenette, and Imagewoof. This attack is realized by constructing *camouflage* datapoints that mask the effect of a poisoned dataset.

1 Introduction

Machine Learning (ML) research traditionally assumes a static pipeline: data is gathered, a model is trained once and subsequently deployed. This paradigm has been challenged by practical deployments, which are more dynamic in nature. After initial deployment more data may be collected, necessitating additional training. Or, as in the *machine unlearning* setting (Cao & Yang, 2015), we may need to produce a model as if certain points were never in the training set to begin with.[1]

While such dynamic settings clearly increase the applicability of ML models, they also make them more vulnerable. Specifically, they open models up to new methods of attack by malicious actors aiming to sabotage the model. In this work, we introduce a new type of data poisoning attack on models that *unlearn* training datapoints. We call these *camouflaged data poisoning attacks*.

The attack takes place in two phases. In the first stage, before the model is trained, the attacker adds a set of carefully designed points to the training data, consisting of a *poison* set and a *camouflage* set. The model's behaviour should be similar whether it is trained on either the training data, or its augmentation with both the poison and camouflage sets. In the second phase, after the model is trained, the attacker triggers an unlearning request to delete the *camouflage* set. That is, the model must be updated to behave as though it were only trained on the training set plus the poison set. At this point, the attack is fully realized, and the model's performance suffers in some way.

While such an attack could harm the model by several metrics, in this paper, we focus on *targeted* poisoning attacks – that is, poisoning attacks where the goal is to misclassify one particular point in the training set. Our contributions are the following:

1. We introduce *camouflaged data poisoning* attacks, demonstrating a new attack vector in dynamic settings including *machine unlearning*.
2. We realize these attacks in the targeted poisoning setting, giving an algorithm based on the gradient-matching approach of Geiping et al. (2021). In order to make the model behavior comparable to as if the poison set were absent, we construct the camouflage set by generating a new set of points that *undoes* the impact of the poison set, an idea which may be of broader interest to the data poisoning community.
3. We demonstrate the efficacy of these attacks on a variety of models (SVMs and neural networks) and datasets (CIFAR-10 (Krizhevsky, 2009), Imagenette (Howard, 2019), and Imagewoof (Howard, 2019)).

[1] A naive solution is to remove said points from the training set and re-train the model from scratch.

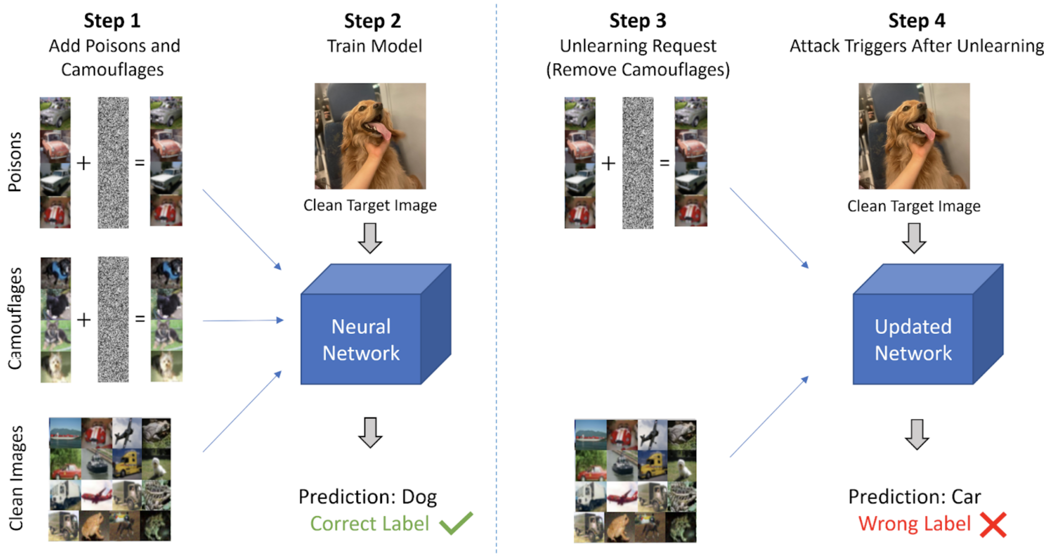

Figure 1: An illustration of a successful camouflaged targeted data poisoning attack. In Step 1, the adversary adds poison and camouflage sets of points to the (clean) training data. In Step 2, the model is trained on the augmented training dataset. It should behave similarly to if trained on only the clean data; in particular, it should correctly classify the targeted point. In Step 3, the adversary triggers an unlearning request to delete the camouflage set from the trained model. In Step 4, the resulting model misclassifies the targeted point.

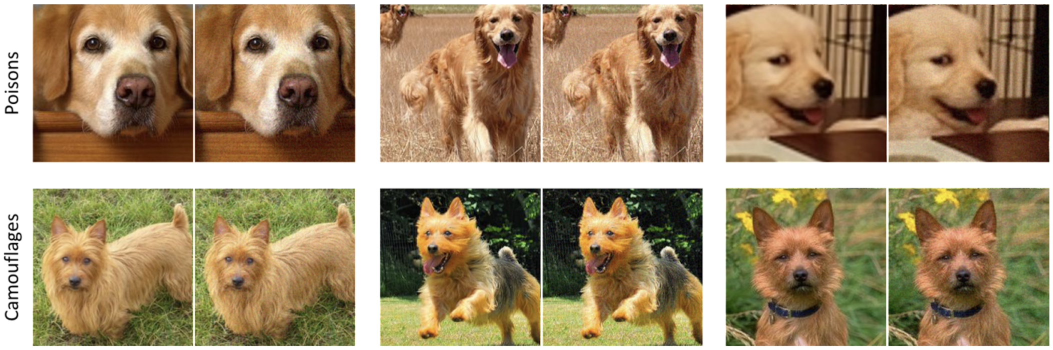

Figure 2: Some representative images from Imagewoof. In each pair, the left figure is from the training dataset, while the right image has been adversarially manipulated. The top and bottom rows are images from the poison and camouflage set, respectively. In all cases, the manipulated images are *clean label* and nearly indistinguishable from the original image.

1.1 Preliminaries

Machine Unlearning. A significant amount of legislation concerning the “right to be forgotten” has recently been introduced by governments around the world, including the European Union’s General Data Protection Regulation (GDPR), the California Consumer Privacy Act (CCPA), and Canada’s proposed Consumer Privacy Protection Act (CPPA). Such legislation requires organizations to delete information they have collected about a user upon request. A natural question is whether that further obligates the organizations to remove that information from downstream machine learning models trained on the data – current guidances (Information Commissioner’s Office, 2020) and precedents (Federal Trade Commission, 2021) indicate that this may be the case. This goal has sparked a recent line of work on *machine unlearning* (Cao & Yang, 2015).

The simplest way to remove a user's data from a trained model is to remove the data from the training set, and then retrain the model on the remainder (also called "retraining from scratch"). This is the ideal way to perform data deletion, as it ensures that the model was never trained on the datapoint of concern. The downside is that retraining may take a significant amount of time in modern machine learning settings. Hence, most work within machine unlearning has studied *fast* methods for data deletion, sometimes relaxing to *approximately* removing the datapoint. A related line of work has focused more on other implications of machine unlearning, particularly the consequences of an adaptive and dynamic data pipeline (Gupta et al., 2021; Marchant et al., 2022). Our work fits into the latter line: we show that the potential to remove points from a trained model can expose a new attack vector. Since retraining from scratch is the ideal result that other methods try to emulate, we focus on unlearning by retraining from scratch, but the same phenomena should still occur when any effective machine unlearning algorithm is applied.

Data Poisoning. In a data poisoning attack, an adversary in some way modifies the training data provided to a machine learning model, such that the model's behaviour at test time is negatively impacted. Our focus is on *targeted data poisoning attacks*, where the attacker's goal is to cause the model to misclassify some specific datapoint in the test set. Other common types of data poisoning attacks include *indiscriminate* (in which the goal is to increase the test error) and *backdoor* (where the goal is to misclassify test points which have been adversarially modified in some small way).

The adversary is typically limited in a couple ways. First, it is common to say that they can only *add* a *small number* of points to the training set. This mimics the setting where the training data is gathered from some large public crowdsourced dataset, and an adversary can contribute a few judiciously selected points of their own. Other choices may include allowing them to *modify* or *delete* points from the training set, but these are less easily motivated. Additionally, the adversary is generally constrained to *clean-label attacks*: if the introduced points were inspected by a human, they should not appear suspicious or incorrectly labeled. We comment that this criteria is subjective and thus not a precise notion, but is nonetheless common in the data poisoning literature, and we use the term as well.

1.2 Related work

The motivation for our work comes from Marchant et al. (2022), who propose a novel poisoning attack on unlearning systems. As mentioned before, the primary goal of many machine unlearning systems is to "unlearn" datapoints quickly, i.e., faster than retraining from scratch. Marchant et al. (2022) craft poisoning schemes via careful noise addition, in order to trigger the unlearning algorithm to retrain from scratch on far more deletion requests than typically required. While both our work and theirs are focused on data poisoning attacks against machine unlearning systems, the adversaries have very different objectives. In our work, the adversary is trying to misclassify a target test point, whereas in theirs, they try to increase the time required to unlearn a point.

In targeted data poisoning, there are a few different types of attacks. The simplest form of attack is *label flipping*, in which the adversary is allowed to flip the labels of the examples (Barreno et al., 2010; Xiao et al., 2012; Paudice et al., 2018). Another type of attack is *watermarking*, in which the feature vectors are perturbed to obtain the desired poisoning effect (Suciu et al., 2018; Shafahi et al., 2018). In both these cases, noticeable changes are made to the label and feature vector, respectively, which would be noticeable by a human labeler. In contrast, *clean label* attacks attempt to make unnoticeable changes to both the feature vector and the label, and are the gold standard for data poisoning attacks (Huang et al., 2020; Geiping et al., 2021). Our focus is on both clean-label poisoning and camouflage sets. While there are also works on indiscriminate (Biggio et al., 2012; Xiao et al., 2015; Muñoz-González et al., 2017; Steinhardt et al., 2017; Diakonikolas et al., 2019; Koh et al., 2022) and backdoor (Gu et al., 2017; Tran et al., 2018; Sun et al., 2019) poisoning attacks, these are beyond the scope of our work, see Goldblum et al. (2020); Cinà et al. (2022) for additional background on data poisoning attacks.

Cao & Yang (2015) initiated the study of machine unlearning through *exact* unlearning, wherein the new model obtained after deleting an example is statistically identical to the model obtained by training on a dataset without the example. A probabilistic notion of unlearning was defined by Ginart et al. (2019), which in turn is inspired from notions in differential privacy (Dwork et al., 2006). Several works studied algorithms for empirical risk minimization (i.e., training loss) (Guo et al., 2020; Izzo et al., 2021; Neel et al., 2021; Ullah et al., 2021), while later works study the effect of machine unlearning on the generalization loss (Gupta et al., 2021; Sekhari et al., 2021). In particular, these works realize that unlearning data points quickly can lead to a drop in test loss, which is the theme of our current work. Several works have considered implementations of machine unlearning in several contexts starting with the work of Bourtoule et al. (2021). These include unlearning in deep neural networks (Golatkar et al., 2020; 2021; Nguyen et al., 2020), random forests (Brophy & Lowd, 2021), large scale language models (Zanella-Béguelin et al., 2020), the tension between unlearning and privacy (Chen et al., 2021), anomaly detection (Du et al., 2019), and even auditing of machine unlearning systems (Sommer et al., 2020).

2 Camouflaged poisoning attacks via unlearning

In this section, we describe various components of the camouflaged poisoning attack, and how it can be realized using machine unlearning.

2.1 Threat model and approach

The camouflaged poisoning attack takes place through interaction between an *attacker* and a *victim*. We assume that the attacker has access to the victim's model architecture,[2] the ability to query gradients on a trained model (which could be achieved, e.g., by having access to the training dataset), and a target sample that it wants to attack. The attacker first sets the stage for the attack by introducing *poison points* and *camouflage points* to the training dataset, which are designed so as to have minimal impact when a model is trained with this modified dataset. At a later time, the attacker triggers the attack by submitting an unlearning request to remove the camouflage points. The victim first trains a machine learning model (e.g., a deep neural network) on the modified training dataset, and then executes the unlearning request by retraining the model from scratch on the left over dataset. The goal of the attacker is to change the prediction of the model on a particular target sample $(x_{\text{target}}, y_{\text{target}})$ previously unseen by the model during training from y_{target} to a desired label $y_{\text{adversarial}}$, while still ensuring good performance over other validation samples. Formally, the interaction between the attacker and the victim is as follows (see Figure 1) :

1. The attacker introduces a small number of poisons samples S_{po} and camouflage samples S_{ca} to a clean training dataset S_{cl}. Define $S_{\text{cpc}} = S_{\text{cl}} + S_{\text{po}} + S_{\text{ca}}$.
2. Victim trains an ML model (e.g., a neural network) on S_{cpc}, and returns the model θ_{cpc}.
3. The attacker submits a request to unlearn the camouflage samples S_{ca}.
4. The victim performs the request, and computes a new model θ_{cp} by retraining from scratch on the left over data samples $S_{\text{cp}} = S_{\text{cl}} + S_{\text{po}}$.

Note that the attack is only realized in Step 4 when the victim executes the unlearning request and retrains the model from scratch on the left over training samples. In fact, in Steps 1-3, the victim's model should behave similarly to as if it were trained on the clean samples S_{cl} only. In particular, the model θ_{cpc} will predict y_{target} on x_{target}, whereas the updated model θ_{cp} will predict $y_{\text{adversarial}}$ on x_{target}. Both models should have comparable validation accuracy. Such an attack is implemented by designing a camouflage set that cancels the effects of the poison set while training, but retraining without the camouflage set exposes the poison set, thus negatively affecting the model.

We highlight that camouflaged attacks may be *more dangerous* than traditional data poisoning attacks, since camouflaged attacks can be triggered by the adversary. That is, the adversary can reveal the attack whenever the submit an unlearning request, whereas for a traditional poisoning attack, the adversary simply plants the attack and must wait for the victim to train the model.

In order to be undetectable, and represent the realistic scenario in which the adversary has limited influence on the model's training data, the attacker is only allowed to introduce a set of points that is much smaller than the size of the clean training dataset (i.e., $|S_{\text{po}}| \ll |S_{\text{cl}}|$ and $|S_{\text{ca}}| \ll |S_{\text{cl}}|$). Throughout the paper and experiments, we denote the relative size of the poison set and camouflage

[2] In Appendix B.6.3, we examine the *transferability* of our proposed attack to unknown victim model, thus relaxing the requirement of knowing the victim's model architecture a priori.

set by $b_p := \frac{|S_{\text{po}}|}{|S_{\text{cl}}|} \times 100$ and $b_c := \frac{|S_{\text{ca}}|}{|S_{\text{cl}}|} \times 100$, respectively. Additionally, the attacker is only allowed to generate poison and camouflage points by altering the base images by less than ε distance in the ℓ_∞ norm (in our experiments $\varepsilon \leq 16$, where the images are represented as an array of pixels in 0 to 255). Thus, the attacker executes a so-called *clean-label* attack, where the corrupted images would be visually indistinguishable from original base images and thus would be given the same label as before by a human data validator. We parameterize a threat model by the tuple (ε, b_c, b_p).

The attacker implements the attack by first generating poison samples, and then generating camouflage samples to cancel their effects. The poison and camouflage points are generated as follows.

Poison points. Poison points are designed so that a network trained on $S_{\text{cp}} = S_{\text{cl}} + S_{\text{po}}$ predicts the label $y_{\text{adversarial}}$ (instead of y_{target}) on a target image x_{target}. While there are numerous data poisoning attacks in the literature, we adopt the state-of-the-art procedure of Geiping et al. (2021) for generating poisons due to its high success rate, efficiency of implementation, and applicability across various models. However, our framework is flexible: in principle, other attacks for the same setting could serve as a drop-in replacement, e.g., the methods of Aghakhani et al. (2021) or Huang et al. (2020), or any method introduced in the future. Suppose that S_{cp} consist of N_1 samples $(x^i, y^i)_{i \leq N_1}$ out of which the first P samples with index $i = 1$ to P belong to the poison set S_{po}.[3] The poison samples are generated by adding small perturbations Δ^i to the base image x^i so as to minimize the loss on the target with respect to the adversarial label, which can be formalized as the following bilevel optimization problem[4]

$$\min_{\Delta \in \Gamma} \ell(f(x_{\text{target}}, \theta(\Delta)), y_{\text{adversarial}}) \quad \text{where} \quad \theta(\Delta) \in \arg\min_\theta \frac{1}{N} \sum_{i \leq N} \ell(f(x^i + \Delta^i, \theta), y^i), \quad (1)$$

where we define the constraint set $\Gamma := \left\{\Delta : \|\Delta\|_\infty \leq \varepsilon \text{ and } \Delta^i = 0 \text{ for all } i > P\right\}$. The main optimization objective in (1) is called the adversarial loss (Geiping et al., 2021).

Camouflage points. Camouflage samples are designed to cancel the effect of the poisons, such that a model trained on $S_{\text{cpc}} = S_{\text{cl}} + S_{\text{po}} + S_{\text{ca}}$ behaves identical to the model trained on S_{cl}, and makes the correct prediction on x_{target}. We formulate this task via a bilevel optimization problem similar to what we did in (1) for generating poisons. Let S_{cpc} consist of N_2 samples $(x^j, y^j)_{j \leq N_2}$ out of which the last C samples with index $j = N_2 - C + 1$ to N_2 belong to the camouflage set S_{ca}. The camouflage points are generated by adding small perturbations Δ^j to the base image x^j so as to minimize the loss on the target with respect to the adversarial label. In particular, we find the appropriate Δ by solving:

$$\min_{\Delta \in \Gamma} \ell(f(x_{\text{target}}, \theta(\Delta)), y_{\text{target}}) \quad \text{where} \quad \theta(\Delta) \in \arg\min_\theta \frac{1}{N_2} \sum_{j \leq N_2} \ell(f(x^j + \Delta^j, \theta), y^j), \quad (2)$$

where we define the constraint set $\Gamma := \left\{\Delta : \|\Delta\|_\infty \leq \varepsilon \text{ and } \Delta^j = 0 \text{ for all } j \leq N_2 - C\right\}$.

2.2 Gradient matching for efficient poison generation (Geiping et al., 2021)

In this section, we discuss the key intuition of Geiping et al. (2021) for efficient poison generation. Our objective is to find perturbations Δ such that when the model is trained on the poisoned samples, it minimizes the adversarial loss in (1) thus making the victim model predict the wrong label $y_{\text{adversarial}}$ on the target sample. However, directly solving (1) is computationally intractable due to bilevel nature of the optimization objective. Instead, one may implicitly minimize the adversarial loss by finding a Δ such that for any model parameter θ,

$$\nabla_\theta(\ell(f(x_{\text{target}}, \theta), y_{\text{adversarial}})) \approx \frac{1}{P} \sum_{i=1}^{P} \nabla_\theta \ell\big(f(x^i + \Delta^i, \theta), y^i\big). \quad (3)$$

In essence, (3) implies that gradient based minimization (e.g., using Adam / SGD) of the training loss on poisoned samples also minimizes the adversarial loss. Thus, training a model on $S_{\text{cl}} + S_{\text{po}}$

[3] This ordering is for notational convenience; naturally, the datapoints are shuffled to preclude the victim simply removing a prefix of the training data.

[4] While (1) focuses on misclassifying a single target point, it is straightforward to extend this to multiple targets by changing the objective to a sum over losses on the target points.

will automatically ensure that the model predicts $y_{\text{adversarial}}$ on the target sample. Unfortunately, computing Δ that satisfies (3) is also intractable as it is required to hold for all values of θ. The key idea of Geiping et al. (2021) to make poison generation efficient is to relax (3) to only be satisfied for a fixed model θ_{cl}−the model obtained by training on the clean dataset S_{cl}. To implement this, Geiping et al. (2021) minimize the cosine-similarity loss between the two gradients defined as:

$$\phi(\Delta, \theta) = 1 - \frac{\left\langle \nabla_\theta \ell(f(x_{\text{target}}, \theta), y_{\text{adversarial}}), \sum_{i=1}^{P} \nabla_\theta \ell(f(x_i + \Delta_i, \theta), y_i) \right\rangle}{\|\nabla_\theta \ell(f(x_{\text{target}}, \theta), y_{\text{adversarial}})\| \|\sum_{i=1}^{P} \nabla_\theta \ell(f(x_i + \Delta_i, \theta), y_i)\|}, \tag{4}$$

Geiping et al. (2021) demonstrated that (4) can be efficiently optimized for many popular large-scale machine learning models and datasets. For completeness, we provide their pseudocode in Algorithm 1 in the Appendix.

2.3 Camouflaging poisoned points

Camouflage images are designed in order to neutralize the effect of the poison images. In this section, we give intuition into what we mean by cancelling the effect of poisons, and provide two procedures for generating camouflages efficiently: label flipping, and gradient matching.

2.3.1 Camouflages via label flipping

Suppose that the underlying task is a binary classification problem with the labels $y \in \{-1, 1\}$, and that the model is trained using linear loss $\ell(f(x,\theta), y) = -yf(x,\theta)$. Then, simply flipping the labels allows one to generate a camouflage set for any given poison set S_{po}. In particular, S_{ca} is constructed as: for every $(x^i, y^i) \in S_{\text{po}}$, simply add $(x^i, -y^i)$ to S_{ca} (i.e., $b_p = b_c$). It is easy to see that for such camouflage points, we have for any θ,

$$\sum_{(x,y)\in S_{\text{cpc}}} \ell(f(x,\theta), y) = -\sum_{(x,y)\in S_{\text{cl}}} yf(x,\theta) - \sum_{i=1}^{P} \left(y^i f(x^i, \theta) + (-y^i) f(x^i, \theta)\right) = \sum_{(x,y)\in S_{\text{cl}}} \ell(f(x,\theta), y).$$

We can also similarly show that the gradients (as well as higher order derivatives) are equal, i.e., $\nabla_\theta \sum_{S_{\text{cpc}}} \ell(f(x,\theta), y) = \nabla_\theta \sum_{S_{\text{cl}}} \ell(f(x,\theta), y)$ for all θ. Thus, training a model on S_{cpc} is equivalent to training it on S_{cl}. In essence, the camouflages have perfectly canceled out the effect of the poisons. We validate the efficacy of this approach via experiments on linear SVM trained with hinge loss (which resembles linear loss when the domain is bounded) on a binary classification problem constructed using CIFAR-10 dataset. We report the results in Table 1 (see Section 3.1.1 for details).

While label flipping is a simple and effective procedure to generate camouflages, it is fairly restrictive. Firstly, label flipping only works for binary classification problems trained with linear loss. Secondly, the attack is not clean label as the camouflage images are generated as $(x^i, -y^i)$ by giving them the opposite label to the ground truth, which can be easily caught by a validator. Lastly, the attack is vulnerable to simple data purification techniques by the victim, e.g., the victim can protect themselves by preprocessing the data to remove all the images that have both the labels ($y = +1$ and $y = -1$) in the training dataset. In the next section, we provide a different procedure to generate clean-label camouflages for general losses and multi-class classification problems.

Attack type	**Attack success**		**Validation Accuracy**		
(ε, b_p, b_c)	Poisoning	Camouflaging	Clean	Poisoned	Camouflaged
LF $(8, 0.2\%, 0.2\%)$	70%	71.5%	81.63	81.73 (± 0.14)	81.74 (± 0.20)
LF $(16, 0.2\%, 0.2\%)$	100%	40%	81.63	81.64 (±0.03)	81.6 (±0.02)
GM $(8, 0.2\%, 0.4\%)$	70%	100%	81.63	81.65 (±0.01)	81.62 (±0.02)
GM $(16, 0.2\%, 0.4\%)$	100%	70%	81.63	81.65 (±0.03)	81.63 (± 0.02)

Table 1: Camouflaged poisoning attack on linear SVM on Binary-CIFAR-10 dataset. The first column lists the threat model (ε, b_p, b_c) and the camouflaging type "LF" for label flipping and "GM" for gradient matching. The implementation details are given in Section 3.1.1. Each experriments is an average of 10 runs with seeds of the form "kkkkkk" where $k \in \{0, \ldots, 9\}$ and the seed 99999.

2.3.2 Gradient matching for generating camouflages

We next discuss our main procedure to generate camouflages, which is based on the gradient matching idea of Geiping et al. (2021). Note that, our objective in (2) is to find Δ such that when the model is trained with the camouflages, it minimizes the original-target loss in (2) (with respect to the original label y_{target}) thus making the victim model predict the correct label on this target sample. Since, (1) is computationally intractable, one may instead try to implicitly minimize the original-target loss by finding a Δ such that for any model parameter θ,

$$\nabla_\theta(\ell(f(x_{\text{target}}, \theta), y_{\text{target}})) \approx \frac{1}{C}\sum_{i=1}^{C} \nabla_\theta \ell\big(f(x^i + \Delta^i, \theta), y^i\big). \tag{5}$$

(5) suggests that minimizing (e.g., using Adam / SGD) on camouflage samples will also minimize the original-target loss, and thus automatically ensure that the model predicts the correct label on the target sample. Unfortunately, (5) is also intractable as it requires the condition to hold for all θ. Building on the work of Geiping et al. (2021), we relax this condition to satisfied only for a fixed model θ_{cp}-the model trained on the dataset $S_{\text{cp}} = S_{\text{cl}} + S_{\text{po}}$. Similar to what we did for generating poison points, we achieve this by minimizing the cosine-similarity loss given by

$$\psi(\Delta, \theta) = 1 - \frac{\big\langle \nabla_\theta \ell(f(x_{\text{target}}, \theta), y_{\text{target}}), \sum_{i=1}^{C} \nabla_\theta \ell(f(x_i + \Delta_i, \theta), y_i)\big\rangle}{\|\nabla_\theta \ell(f(x_{\text{target}}, \theta), y_{\text{target}})\| \|\sum_{i=1}^{C} \nabla_\theta \ell(f(x_i + \Delta_i, \theta), y_i)\|}. \tag{6}$$

Implementation details. We minimize (6) using the Adam optimizer (Kingma & Ba, 2015) with a fixed step size of 0.1. In order to increase the robustness of camouflage generation, we do R restarts (where $R \leq 10$). In each restart, we first initialize Δ randomly such that $\|\Delta\|_\infty \leq \varepsilon$ and perform M steps of Adam optimization to minimize $\psi(\Delta, \theta_{\text{cp}})$. Each optimization step only requires a single differentiation of the objective ψ with respect to Δ, and can be implemented efficiently. After each step, we project back the updated Δ into the constraint set Γ so as to maintain the property that $\|\Delta\|_\infty \leq \varepsilon$. After doing R restarts, we choose the best round by finding Δ_* with the minimum $\psi(\Delta_\star, \theta_{\text{cp}})$. We provide the pseudocode in Algorithm 2 in the appendix.

3 Experimental Evaluation

In this section, we give details into our experimental setup. We generate poison points by running Algorithm 1, and camouflage points by running Algorithm 2 with $R = 1$ and $M = 250$.[5] Each experiment is repeated K times by setting a different seed each time, which fixes the target image, poison class, camouflage class, base poison images and base camouflage images. Due to limited computation resources, we typically set $K \in \{3, 5, 8, 10\}$ depending on the dataset and report the mean and standard deviation across different trials. We say that *poisoning* was successful if the model trained on $S_{\text{cp}} = S_{\text{cl}} + S_{\text{po}}$ predicts the label $y_{\text{adversarial}}$ on the target image. Furthermore, we say that *camouflaging* was successful if the model trained on $S_{\text{cpc}} = S_{\text{po}} + S_{\text{cl}} + S_{\text{ca}}$ predicts back the correct label y_{target} on the target image, provided that poisoning was successful. A camouflaged poisoning attack is successful if both poisoning and camouflaging were successful.

For the ease of replication, we provide the code for our experiments with the supplementary material (see Appendix B.2 for details).

3.1 Evaluations on Cifar-10

We extensively evaluate our camouflaged poisoning attack on models trained on the CIFAR-10 dataset (Krizhevsky, 2009). CIFAR-10 is a multiclass classification problem with 10 classes, with 6,000 color images in each class (5,000 training + 1,000 test) of size 32×32. We follow the standard split into 50,000 training images and 10,000) validation / test images.

[5] We note that we diverge slightly from the threat model described above, in that the adversary *modifies* rather than introduces new points. We do this for convenience, but we do not anticipate the results would qualitatively change.

3.1.1 Support Vector Machines

In order to perform evaluations on SVM, we first convert the CIFAR-10 dataset into a binary classification dataset (which we term as Binary-CIFAR-10) by merging the 10 classes into two groups: `animal` ($y = +1$) and `machine` ($y = -1$). Images (in the training and the test dataset) that were originally labeled (*bird, cat, deer, dog, frog, horse*) are instead labeled `animal`, and the remaining images, with original labels (*airplane, cars, ship, truck*), are labeled `machine`.

We train a linear SVM (no kernel was used) with the hinge loss: $\ell(f(x,\theta), y) = \max\{0, 1 - yf(x,\theta)\}$. The training was done using the `svm.LinearSVC` class from Scikit-learn (Pedregosa et al., 2011) on a single CPU. In the pre-processing stage, each image in the training dataset was normalized to have ℓ_2-norm 1. Each training on Binary-CIFAR-10 dataset took 25 - 30 seconds. In order to generate the poison points, we first use `torch.autograd` to compute the cosine-similarity loss (4), and then optimize it using Adam optimizer with learning rate 0.001. Each poison and camouflage generation took about 40 - 50 seconds (for $b_p = b_c = 0.2\%$). We evaluate both label flipping and gradient matching to generate camouflages, and different threat models (ε, b_p, b_c); the results are reported in Table 1. For each of our experiments we chose $K = 10$ seeds. Each trained model had validation accuracy of around 81.63% on the clean dataset S_{cl}, which did not change significantly when we retrained after adding poison samples and / or camouflage samples. Note that the efficacy of the camouflaged poisoning attack was more than 70% in most of the experiments. We provide a sample of the generated poisons and camouflages in Figure 4 in the appendix.

3.1.2 Neural Networks

We perform extensive evaluations on the multiclass CIFAR-10 classification task with various popular large scale neural networks architectures including VGG-11, VGG-16 (Simonyan & Zisserman, 2015), ResNet-18, ResNet-34, ResNet-50 (He et al., 2016), and MobileNetV2 (Sandler et al., 2018).

Each model is trained with cross-entropy loss $\ell(f(x,\theta), y) = -\log(\Pr(y = f(x,\theta)))$ on a single GPU using PyTorch (Paszke et al., 2019), and using mini-batch SGD with weight decay 5e-4, momentum 0.9, learning rate 0.01, batch size 100, and 40 epochs over the training dataset. Each training run took about 45 minutes. The poison and camouflage sets were generated using gradient matching by first defining the cosine-similarity loss using `torch.autograd` and then minimizing it using Adam with a learning rate of 0.1. Each poison/camouflage generation took about 1.5 hours.

We report the efficacy of our camouflaged poisoning attack across different models and threat models (ε, b_p, b_c) in Figure 3; also see Appendix B.4 for detailed results and performance drops on the validation dataset after adding poison and camouflage set. Each model was trained to have validation accuracy between 81-87% (depending on the architecture), which changed minimally when the model was retrained with poison and camouflage samples. Poisoning was successful at least 80% of the time in most of the experiments. Camouflaging was successful at least 70% of the time for VGG-11, VGG-16, Resnet-18, and Resnet-34 but was not as successful for MobileNetV2 and Resnet-50. Furthermore, camouflaging succeeded at least 75% of times when $b_c = b_p$, but did not perform as well when we set $b_p > b_c$ in the thread model (more poison images than camouflage images).

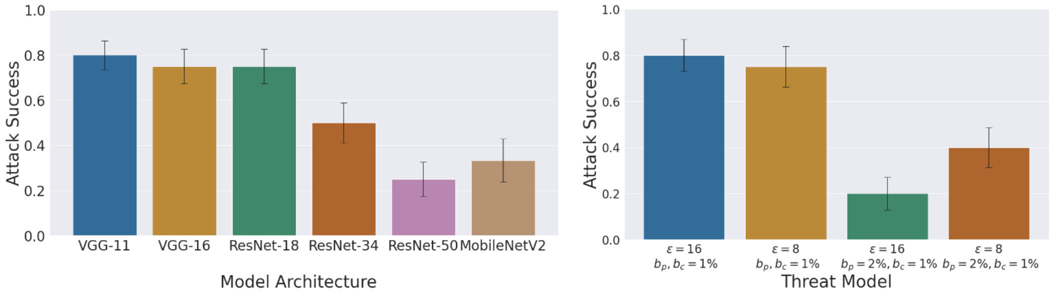

Figure 3: Efficacy of the proposed camouflaged poisoning attack on CIFAR-10 dataset. The left plot gives the success for the threat model $\varepsilon = 16, b_p = 0.6\%, b_c = 0.6\%$ across different neural network architectures. The right plot gives the success for ResNet-18 architecture across different threat models. See Appendix B.4 for the experiment details.

3.2 Evaluations on Imagenette and Imagewoof

We evaluate the efficacy of our attack vector on the challenging multiclass classification problem on the Imagenette and Imagewoof datasets (Howard, 2019). Imagenette is a subset of 10 classes (*Tench, English springer, Cassette player, Chain saw, Building/church, French horn, Truck, Gas pump, Golf ball, Parachute*) from the Imagenet dataset (Russakovsky et al., 2015). The Imagenette dataset consists of around 900 images of various sizes for each class. In total, we have 13394 images which are divided into a training dataset of size 9469 and test dataset of size 3925. To perform training, all images are resized and centrally cropped down to 224 × 224 pixels.

Dataset	**Model**	**Threat Model**			**Attack Success**	
		ε	b_p	b_c	Poisoning	Camouflaging
Imagenette	VGG-16	16	6.3%	6.3%	25%	100%
Imagenette	Resnet-18	16	6.3%	6.3%	40%	50%
Imagewoof	Resnet-18	16	6.6%	6.6%	50%	75%

Table 2: Evaluation of camouflaged poisoning attack on Imagenette and Imagewoof datasets over 5 seeds (with 1 restart per seed). Note that camouflaging succeeded in most of the experiments in which poisoning succeeded. Prior works (e.g., Geiping et al. (2021)) set a large number of restarts R, and then choose the most effective attack among them. Due to computational constraints, we ran only one restart (i.e., $R = 1$) for each experiment. Given additional computational resources, we could inflate the success rate of both the poisoning and camouflaging.

Imagewoof (Howard, 2019) is another subset of Imagenet dataset consisting of 10 classes (*Shih-Tzu, Rodesian Ridgeback, Beagle, English Foxhound, Border Terrier, Austrailian Terrier, Golden Retriever, Old English Sheep Dog, Samoyed, Dingo*). Imagewoof consists of around 900 images of various sizes for each class, and in total 12954 images which are divided into a training dataset of size 9025 and test dataset of size 3929. Similar to Imagenette, we resize all images and crop to the central 224 × 224 pixels before training.

We evaluate our camouflaged poisoning attack on two different neural network architectures-VGG-16 and ResNet-18, and different threat models (ε, b_p, b_c) listed in Table 3.2. Each model is trained on a single GPU with cross-entropy loss, that is minimized using SGD algorithm with weight decay 5e-4, momentum 0.9 and batch size 20. We start with a learning rate of 0.01, and exponentially decay it with $\gamma = 0.9$ after every epoch, for a total of 50 epochs over the training dataset. The poisons and camouflages were generated using gradient matching by first defining the cosine-similarity loss using `torch.autograd` and then optimizing it using Adam optimizer with learning rate 0.1. In our experiments, camouflaging was successful for at least 50% of the time when poisoning was successful. However, because we modified about 13% of the training dataset when adding poisons / camouflages, we observe that the fluctuation in the model's validation accuracy can be up to 7% for both Imagenette and Imagewoof, as expected on making such a large change in the training set.

Additional experiments. In Appendix B.6, we provide additional experiments on CIFAR-10 showing that our attack is robust to data augmentation, and successfully transfers when the victim model is different from the model on which poison and camouflage samples were generated.

Conclusion and discussion. We demonstrated a new attack vector, *camouflaged poisoning attacks*, against machine learning pipelines where training points can be *unlearned*. This shows that as we introduce new functionality to machine learning systems, we must be aware of novel threats that emerge. We outline a few interesting directions for further research: It is important to understand how to *defend* against camouflaged attacks. As observed by Geiping et al. (2021), it is unlikely that differential privacy (Dwork et al., 2006) would be an effective defense, as preventing attacks in the non-camouflaged setting incurs too significant a loss in accuracy. Another direction is to reduce the knowledge needed by the adversary, thereby creating stronger attacks. E.g., while our setting requires grey-box knowledge, one could instead consider a black-box model to attack ML APIs. Finally, it is interesting to determine what other types of threats can be camouflaged, e.g., indiscriminate or backdoor poisoning attacks. Beyond exploring this new attack vector, it is also independently interesting to understand how one can neutralize the effect of an attack by *adding* points.

Reproducibility Statement

For the purposes of reproducibility, we include our code in the supplement. Descriptions of the various files are given in Appendix B.2. Hyperparameters and experimental details for all experiments are provided in Section 3. Finally, we report random seeds, target points and classes, poison and camouflage classes for all experiments in Appendix B.3.

References

Hojjat Aghakhani, Dongyu Meng, Yu-Xiang Wang, Christopher Kruegel, and Giovanni Vigna. Bullseye polytope: A scalable clean-label poisoning attack with improved transferability. In *2021 IEEE European Symposium on Security and Privacy (EuroS&P)*, pp. 159–178. IEEE, 2021.

Marco Barreno, Blaine Nelson, Anthony D Joseph, and J Doug Tygar. The security of machine learning. *Machine Learning*, 81(2):121–148, 2010.

Battista Biggio, Blaine Nelson, and Pavel Laskov. Poisoning attacks against support vector machines. In *Proceedings of the 29th International Conference on Machine Learning*, ICML '12, pp. 1467–1474. JMLR, Inc., 2012.

Lucas Bourtoule, Varun Chandrasekaran, Christopher A Choquette-Choo, Hengrui Jia, Adelin Travers, Baiwu Zhang, David Lie, and Nicolas Papernot. Machine unlearning. In *proceedings of the 42nd IEEE Symposium on Security and Privacy*, SP '21, Washington, DC, USA, 2021. IEEE Computer Society.

Jonathan Brophy and Daniel Lowd. Machine unlearning for random forests. In *Proceedings of the 38th International Conference on Machine Learning*, ICML '21, pp. 1092–1104. JMLR, Inc., 2021.

Yinzhi Cao and Junfeng Yang. Towards making systems forget with machine unlearning. In *Proceedings of the 36th IEEE Symposium on Security and Privacy*, SP '15, pp. 463–480, Washington, DC, USA, 2015. IEEE Computer Society.

Min Chen, Zhikun Zhang, Tianhao Wang, Michael Backes, Mathias Humbert, and Yang Zhang. When machine unlearning jeopardizes privacy. In *Proceedings of the 2021 ACM SIGSAC Conference on Computer and Communications Security*, pp. 896–911, 2021.

Antonio Emanuele Cinà, Kathrin Grosse, Ambra Demontis, Sebastiano Vascon, Werner Zellinger, Bernhard A Moser, Alina Oprea, Battista Biggio, Marcello Pelillo, and Fabio Roli. Wild patterns reloaded: A survey of machine learning security against training data poisoning. *arXiv preprint arXiv:2205.01992*, 2022.

Ilias Diakonikolas, Gautam Kamath, Daniel M. Kane, Jerry Li, Jacob Steinhardt, and Alistair Stewart. Sever: A robust meta-algorithm for stochastic optimization. In *Proceedings of the 36th International Conference on Machine Learning*, ICML '19, pp. 1596–1606. JMLR, Inc., 2019.

Min Du, Zhi Chen, Chang Liu, Rajvardhan Oak, and Dawn Song. Lifelong anomaly detection through unlearning. In *Proceedings of the 2019 ACM SIGSAC Conference on Computer and Communications Security*, pp. 1283–1297, 2019.

Cynthia Dwork, Frank McSherry, Kobbi Nissim, and Adam Smith. Calibrating noise to sensitivity in private data analysis. In *Proceedings of the 3rd Conference on Theory of Cryptography*, TCC '06, pp. 265–284, Berlin, Heidelberg, 2006. Springer.

Federal Trade Commission. California company settles ftc allegations it deceived consumers about use of facial recognition in photo storage app, January 2021.

Jonas Geiping, Liam Fowl, W Ronny Huang, Wojciech Czaja, Gavin Taylor, Michael Moeller, and Tom Goldstein. Witches' brew: Industrial scale data poisoning via gradient matching. In *Proceedings of the 9th International Conference on Learning Representations*, ICLR '21, 2021.

General Data Protection Regulation. Regulation (EU) 2016/679 of the European parliament and of the council of 27 April 2016, 2016.

Antonio Ginart, Melody Guan, Gregory Valiant, and James Y Zou. Making AI forget you: Data deletion in machine learning. In *Advances in Neural Information Processing Systems 32*, NeurIPS '19, pp. 3518–3531. Curran Associates, Inc., 2019.

Aditya Golatkar, Alessandro Achille, and Stefano Soatto. Eternal sunshine of the spotless net: Selective forgetting in deep networks. In *Proceedings of the 2020 IEEE Computer Society Conference on Computer Vision and Pattern Recognition*, CVPR '20, pp. 9304–9312, Washington, DC, USA, 2020. IEEE Computer Society.

Aditya Golatkar, Alessandro Achille, Avinash Ravichandran, Marzia Polito, and Stefano Soatto. Mixed-privacy forgetting in deep networks. In *Proceedings of the 2021 IEEE Computer Society Conference on Computer Vision and Pattern Recognition*, CVPR '21, pp. 792–801. IEEE Computer Society, 2021.

Micah Goldblum, Dimitris Tsipras, Chulin Xie, Xinyun Chen, Avi Schwarzschild, Dawn Song, Aleksander Madry, Bo Li, and Tom Goldstein. Dataset security for machine learning: Data poisoning, backdoor attacks, and defenses. *arXiv preprint arXiv:2012.10544*, 2020.

Tianyu Gu, Brendan Dolan-Gavitt, and Siddharth Garg. Badnets: Identifying vulnerabilities in the machine learning model supply chain. *arXiv preprint arXiv:1708.06733*, 2017.

Chuan Guo, Tom Goldstein, Awni Hannun, and Laurens Van Der Maaten. Certified data removal from machine learning models. In *Proceedings of the 37th International Conference on Machine Learning*, ICML '20, pp. 3832–3842. JMLR, Inc., 2020.

Varun Gupta, Christopher Jung, Seth Neel, Aaron Roth, Saeed Sharifi-Malvajerdi, and Chris Waites. Adaptive machine unlearning. In *Advances in Neural Information Processing Systems 34*, NeurIPS '21, pp. 16319–16330. Curran Associates, Inc., 2021.

Kaiming He, Xiangyu Zhang, Shaoqing Ren, and Jian Sun. Deep residual learning for image recognition. In *Proceedings of the 2016 IEEE Computer Society Conference on Computer Vision and Pattern Recognition*, CVPR '16, pp. 770–778, Washington, DC, USA, 2016. IEEE Computer Society.

Jeremy Howard. Imagenette, 2019. URL https://github.com/fastai/imagenette/.

W Ronny Huang, Jonas Geiping, Liam Fowl, Gavin Taylor, and Tom Goldstein. Metapoison: Practical general-purpose clean-label data poisoning. In *Advances in Neural Information Processing Systems 33*, NeurIPS '20, pp. 12080–12091. Curran Associates, Inc., 2020.

Information Commissioner's Office. Guidance on the ai auditing framework, February 2020.

Zachary Izzo, Mary Anne Smart, Kamalika Chaudhuri, and James Zou. Approximate data deletion from machine learning models: Algorithms and evaluation. In *Proceedings of the 24th International Conference on Artificial Intelligence and Statistics*, AISTATS '21, pp. 2008–2016. JMLR, Inc., 2021.

Diederik P Kingma and Jimmy Ba. Adam: A method for stochastic optimization. In *Proceedings of the 3rd International Conference on Learning Representations*, ICLR '15, 2015.

Pang Wei Koh, Jacob Steinhardt, and Percy Liang. Stronger data poisoning attacks break data sanitization defenses. *Machine Learning*, 111(1):1–47, 2022.

Alex Krizhevsky. Learning multiple layers of features from tiny images, 2009.

Neil G Marchant, Benjamin IP Rubinstein, and Scott Alfeld. Hard to forget: Poisoning attacks on certified machine unlearning. In *Proceedings of the Thirty-Sixth AAAI Conference on Artificial Intelligence*, volume 36 of *AAAI '22*, pp. 7691–7700, 2022.

Luis Muñoz-González, Battista Biggio, Ambra Demontis, Andrea Paudice, Vasin Wongrassamee, Emil C Lupu, and Fabio Roli. Towards poisoning of deep learning algorithms with back-gradient optimization. In *Proceedings of the 10th ACM workshop on artificial intelligence and security*, pp. 27–38, 2017.

Seth Neel, Aaron Roth, and Saeed Sharifi-Malvajerdi. Descent-to-delete: Gradient-based methods for machine unlearning. In *Proceedings of the 32nd International Conference on Algorithmic Learning Theory*, ALT '21. JMLR, Inc., 2021.

Quoc Phong Nguyen, Bryan Kian Hsiang Low, and Patrick Jaillet. Variational bayesian unlearning. *Advances in Neural Information Processing Systems*, 33:16025–16036, 2020.

Adam Paszke, Sam Gross, Francisco Massa, Adam Lerer, James Bradbury, Gregory Chanan, Trevor Killeen, Zeming Lin, Natalia Gimelshein, Luca Antiga, Alban Desmaison, Andreas Köpf, Edward Yang, Zach DeVito, Martin Raison, Alykhan Tejani, Sasank Chilamkurthy, Benoit Steiner, Lu Fang, Junjie Bai, and Soumith Chintala. PyTorch: An imperative style, high-performance deep learning library. In *Advances in Neural Information Processing Systems 32*, NeurIPS '19, pp. 8026–8037. Curran Associates, Inc., 2019.

Andrea Paudice, Luis Muñoz-González, and Emil C Lupu. Label sanitization against label flipping poisoning attacks. In *Joint European conference on machine learning and knowledge discovery in databases*, pp. 5–15. Springer, 2018.

Fabian Pedregosa, Gaël Varoquaux, Alexandre Gramfort, Vincent Michel, Bertrand Thirion, Olivier Grisel, Mathieu Blondel, Peter Prettenhofer, Ron Weiss, Vincent Dubourg, Jake Vanderplas, Alexandre Passos, David Cournapeau, Matthieu Brucher, Matthieu Perrot, and Édouard Duchesnay. Scikit-learn: Machine learning in Python. *Journal of Machine Learning Research*, 12(85): 2825–2830, 2011.

Olga Russakovsky, Jia Deng, Hao Su, Jonathan Krause, Sanjeev Satheesh, Sean Ma, Zhiheng Huang, Andrej Karpathy, Aditya Khosla, Michael Bernstein, et al. Imagenet large scale visual recognition challenge. *International journal of computer vision*, 115(3):211–252, 2015.

Mark Sandler, Andrew Howard, Menglong Zhu, Andrey Zhmoginov, and Liang-Chieh Chen. MobileNetV2: Inverted residuals and linear bottlenecks. In *Proceedings of the 2018 IEEE Computer Society Conference on Computer Vision and Pattern Recognition*, CVPR '18, pp. 4510–4520, Washington, DC, USA, 2018. IEEE Computer Society.

Ayush Sekhari, Jayadev Acharya, Gautam Kamath, and Ananda Theertha Suresh. Remember what you want to forget: Algorithms for machine unlearning. In *Advances in Neural Information Processing Systems 34*, NeurIPS '21, pp. 18075–18086. Curran Associates, Inc., 2021.

Ali Shafahi, W Ronny Huang, Mahyar Najibi, Octavian Suciu, Christoph Studer, Tudor Dumitras, and Tom Goldstein. Poison frogs! targeted clean-label poisoning attacks on neural networks. *Advances in neural information processing systems*, 31, 2018.

Karen Simonyan and Andrew Zisserman. Very deep convolutional networks for large-scale visual recognition. In *Proceedings of the 3rd International Conference on Learning Representations*, ICLR '15, 2015.

David Marco Sommer, Liwei Song, Sameer Wagh, and Prateek Mittal. Towards probabilistic verification of machine unlearning. *arXiv preprint arXiv:2003.04247*, 2020.

Jacob Steinhardt, Pang Wei W Koh, and Percy S Liang. Certified defenses for data poisoning attacks. In *Advances in Neural Information Processing Systems 30*, NeurIPS '17, pp. 3520–3532. Curran Associates, Inc., 2017.

Octavian Suciu, Radu Marginean, Yigitcan Kaya, Hal Daume III, and Tudor Dumitras. When does machine learning {FAIL}? generalized transferability for evasion and poisoning attacks. In *27th USENIX Security Symposium (USENIX Security 18)*, pp. 1299–1316, 2018.

Ziteng Sun, Peter Kairouz, Ananda Theertha Suresh, and H Brendan McMahan. Can you really backdoor federated learning? *arXiv preprint arXiv:1911.07963*, 2019.

Brandon Tran, Jerry Li, and Aleksander Madry. Spectral signatures in backdoor attacks. In *Advances in Neural Information Processing Systems 31*, NeurIPS '18, pp. 8011–8021. Curran Associates, Inc., 2018.

Enayat Ullah, Tung Mai, Anup Rao, Ryan A Rossi, and Raman Arora. Machine unlearning via algorithmic stability. In *Conference on Learning Theory*, pp. 4126–4142. PMLR, 2021.

Han Xiao, Huang Xiao, and Claudia Eckert. Adversarial label flips attack on support vector machines. In *ECAI 2012*, pp. 870–875. IOS Press, 2012.

Huang Xiao, Battista Biggio, Blaine Nelson, Han Xiao, Claudia Eckert, and Fabio Roli. Support vector machines under adversarial label contamination. *Neurocomputing*, 160:53–62, 2015.

Santiago Zanella-Béguelin, Lukas Wutschitz, Shruti Tople, Victor Rühle, Andrew Paverd, Olga Ohrimenko, Boris Köpf, and Marc Brockschmidt. Analyzing information leakage of updates to natural language models. In *Proceedings of the 2020 ACM SIGSAC Conference on Computer and Communications Security*, pp. 363–375, 2020.

A Poison generation algorithm

Algorithm 1 Gradient Matching to generate poisons (Geiping et al., 2021)

```
Require: Clean network $f(\cdot;\theta_{\text{clean}})$ trained on uncorrupted base images $S_{\text{cl}}$, a target
    $(x_{\text{target}}, y_{\text{target}})$ and an adversarial label $y_{\text{adversarial}}$, Poison budget $P$, perturbation bound $\varepsilon$,
    number of restarts $R$, optimization steps $M$
Collect a dataset $S_{\text{po}} = \left\{x^i, y^i\right\}_{i=1}^{P}$ of $P$ many images whose true label is $y_{\text{adversarial}}$.
for $r = 1, \ldots R$ restarts do
    Randomly initialize perturbations $\Delta$ s.t. $\|\Delta\|_\infty \leq \varepsilon$.
    for $k = 1, \ldots, M$ optimization steps do
        Compute the loss $\phi(\Delta, \theta_{\text{clean}})$ as in (4) using the base poison images in $S_{\text{po}}$.
        Update $\Delta$ using an Adam update to minimize $\phi$, and project onto the constraint set $\Gamma$.
    end for
    Amongst the $R$ restarts, choose the $\Delta_*$ with the smallest value of $\phi(\Delta_*, \theta_{\text{clean}})$.
end for
Return the poisoned set $S_{\text{po}} = \left\{x^i + \Delta_*^i, y^i\right\}_{i=1}^{P}$.
```

Algorithm 2 Gradient Matching to generate camouflages

```
Require: Network $f(\cdot\,;\theta_{\text{cp}})$ trained on $S_{\text{cl}} + S_{\text{po}}$ , the target $(x_{\text{target}}, y_{\text{target}})$, Camouflage budget
    $C$, perturbation bound $\varepsilon$, number of restarts $R$, optimization steps $M$
Collect a dataset $S_{\text{ca}} = \left\{x^j, y^j\right\}_{j=1}^{C}$ of $C$ many images whose true label is $y_{\text{target}}$.
for $r = 1, \ldots R$ restarts do
    Randomly initialize perturbations $\Delta$ s.t. $\|\Delta\|_\infty \leq \varepsilon$.
    for $k = 1, \ldots, M$ optimization steps do
        Compute the loss $\psi(\Delta, \theta_{\text{cp}})$ as in (4) using the base camouflage images in $S_{\text{ca}}$.
        Update $\Delta$ using an Adam update to minimize $\psi$, and project onto the constraint set $\Gamma$.
    end for
    Amongst the $R$ restarts, choose the $\Delta_*$ with the smallest value of $\psi(\Delta_*, \theta_{\text{cp}})$.
end for
Return the poisoned set $S_{\text{ca}} = \left\{x^j + \Delta_*^j, y^j\right\}_{j=1}^{C}$.
```

B Experiment details

B.1 Hardware

All our experiments were executed on Google Colab with a Google Colab Pro+ subscription.

B.2 Code

We provide code for our experiments as ready-to-deploy Colab notebooks (as well as Python files). In the supplementary material, the code can be found in:

1. `SVM_Binay_cifar10_code_submission.ipynb`: Experiments for Binary-CIFAR-10 dataset with linear SVM.
2. `Neural_network_Cifar10_code_submission.ipynb`: Experiments for CIFAR-10 dataset with various neural network models.
3. `Neural_network_Imagenette_Imagewoof_code_submission.ipynb`: Experiments for Imagenette / Imagewoof dataset with various neural network models.

B.3 Experimental Setup

For the ease of replication, we report the corresponding poison class, target class, camouflage class and Target ID for various seeds in different experiments.

Random Seed	Target Class	Poison Class	Camouflage Class	Target ID
2000000000	Deer	Bird	Deer	9621
2000000001	Cat	Horse	Cat	1209
2000000011	Frog	Bird	Frog	6503
2000000111	Bird	Cat	Bird	124
2000001111	Plane	Deer	Plane	7649
2000011111	Cat	Dog	Cat	4423
2000111111	Truck	Car	Truck	8117
2001111111	Bird	Truck	Bird	3686
2011111111	Cat	Bird	Cat	642
2111111111	Frog	Ship	Frog	97

Table 3: Target, poison and camouflage class corresponding to different initial random seeds used for CIFAR-10 experiments. The reported Target ID is relative to the CIFAR-10 validation dataset.

Random Seed	Target Class	Poison Class	Camouflage Class	Target ID
2000000000	Building	Cassette player	Building	1559
2000000001	Chain saw	Gas pump	Chain saw	1266
2000000011	Truck	Cassette player	Truck	2460
2000000111	Cassette player	Chain saw	Cassette player	792
2000001111	Tench	Building	Tench	2500
2000011111	Chain saw	French horn	Chain saw	1162
2000111111	Parachute	English springer	Parachute	3826
2001111111	Cassette player	Parachute	Cassette player	1121
2011111111	Chain saw	Cassette player	Chain saw	1198
2111111111	Truck	Golf ball	Truck	2343

Table 4: Target class, poison class and camouflage class corresponding to different random seeds used for Imagenette experiments. The reported target ID is relative to the Imagenette validation set.

Random Seed	Target Class	Poison Class	Camouflage Class	Target ID
2000000000	Border Terrier	Beagle	Border Terrier	1493
2000000001	English Foxhound	Old English Sheep Dog	English Foxhound	1362
2000000011	Golden Retriever	Beagle	Golden Retriever	2399
2000000111	Beagle	English Foxhound	Beagle	827
2000001111	Shih-Tzu	Border Terrier	Shih-Tzu	250
2000011111	English Foxhound	Austrailian Terrier	English Foxhound	1405
2000111111	Dingo	Rodesian Ridgeback	Dingo	3810
2001111111	Beagle	Dingo	Beagle	1204
2011111111	English Foxhound	Beagle	English Foxhound	1294
2111111111	Golden Retriever	Samoeyed	Golden Retriever	2282

Table 5: Target class, poison class and camouflage class corresponding to different random seeds used for Imagewoof experiments. The reported target ID is relative to the Imagewoof validation set.

B.4 Additional details on CIFAR-10 Experiments

We elaborate on the results reported in Figure 3. In Table 6, we report the efficacy of the proposed camouflaged poisoning attack on different neural network architectures where the threat model is given by $\varepsilon = 16, b_p = 0.6\%, b_c = 0.6\%$. The reported results are an average over 5 seeds from 2000000000-2000001111. In the first column under attack success, we report the number of times poisoning was successful amongst the run trials, and in the second column, we report the number of times camouflaging was successful for the trials for which poisoning was successful.

In Table 7, we report the success of the proposed attack when we change the threat model, but fix the network architecture to be ResNet-18. Each experiment was repeated times 5 times with 8 restarts each time, and the mean success rate is reported. These experiments were conducted with 5 seeds from 2000011111-2111111111.

Network Architecture	**Attack success**		**Validation Accuracy**		
	Poisoning	Camouflaging	Clean	Poisoned	Camouflaged
VGG-11	100%	80%	85.01	85.03 (± 0.37)	85.10 (± 0.29)
VGG-16	80%	75%	87.68	87.42 (± 0.17)	87.45 (± 0.26)
ResNet-18	80%	75%	82.13	81.88 (± 0.15)	81.80 (± 0.12)
ResNet-34	80%	50%	82.45	82.61 (± 0.30)	83.12 (± 0.93)
ResNet-50	80%	25%	81.02	81.76 (± 0.13)	84.62 (± 0.71)
MobileNetV2	60%	33%	82.79	83.26 (± 0.25)	85.47 (± 0.27)

Table 6: Evaluating our proposed camouflaged poisoning attack on various model architectures on the CIFAR-10 dataset with the threat model $\varepsilon = 16, b_p = 0.6\%, b_c = 0.6\%$.

Threat model			**Attack success**		**Validation Accuracy**		
ε	b_p	b_c	Poisoning	Camouflaging	Clean	Poisoned	Camouflaged
16	1%	1%	100%	80%	82.13	81.98 (± 0.16)	82.12 (± 0.21)
8	1%	1%	80%	75%	82.13	82.21 (± 0.21)	82.09 (± 0.23)
16	2%	1%	100%	20%	82.13	82.31 (± 0.26)	82.19 (± 0.24)
8	2%	1%	100%	40%	82.13	82.43 (± 0.30)	82.34 (± 0.27)

Table 7: Evaluating our proposed camouflaged poisoning attack on various threat models with CIFAR-10 dataset trained on ResNet-18.

B.5 VISUALIZATIONS

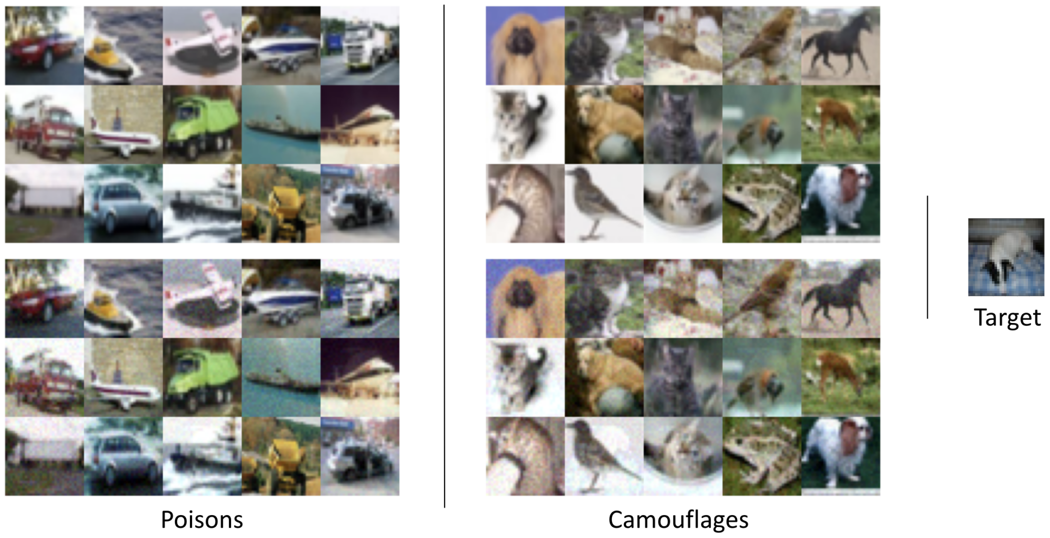

Figure 4: Visualization of poisons and camouflages on Binary-CIFAR-10 dataset (*animal* vs *machine* classification). The top row shows the original images and the bottom row shows the corresponding poisoned / camouflaged images (with the added Δ). The shown images were generated for a camouflaged poisoning attack on SVM, with Seed = 555555, ε = 16, b_p = 0.2, b_c = 0.4 and the target ID 6646.

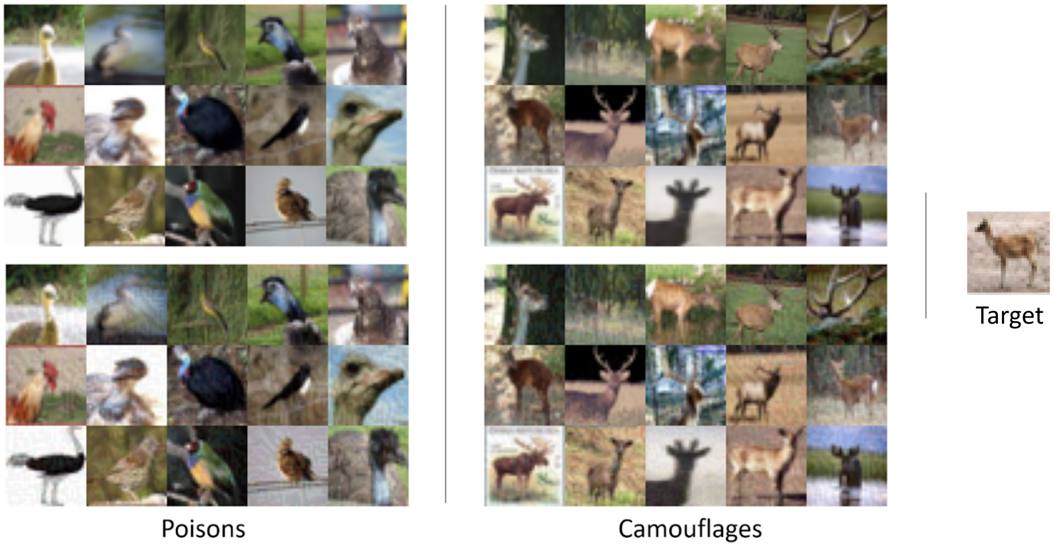

Figure 5: Visualization of poisons and camouflages on CIFAR-10 dataset (multiclass classification task). The top row shows the original images and the bottom row shows the corresponding poisoned / camouflaged images (with the added Δ). The shown images were generated for a camouflaged poisoning attack on ResNet-18, with Seed = 2000000000, ε = 8, b_p = 0.2, b_c = 0.4, poison class *bird*, target class *deer*, and the target ID 9621.

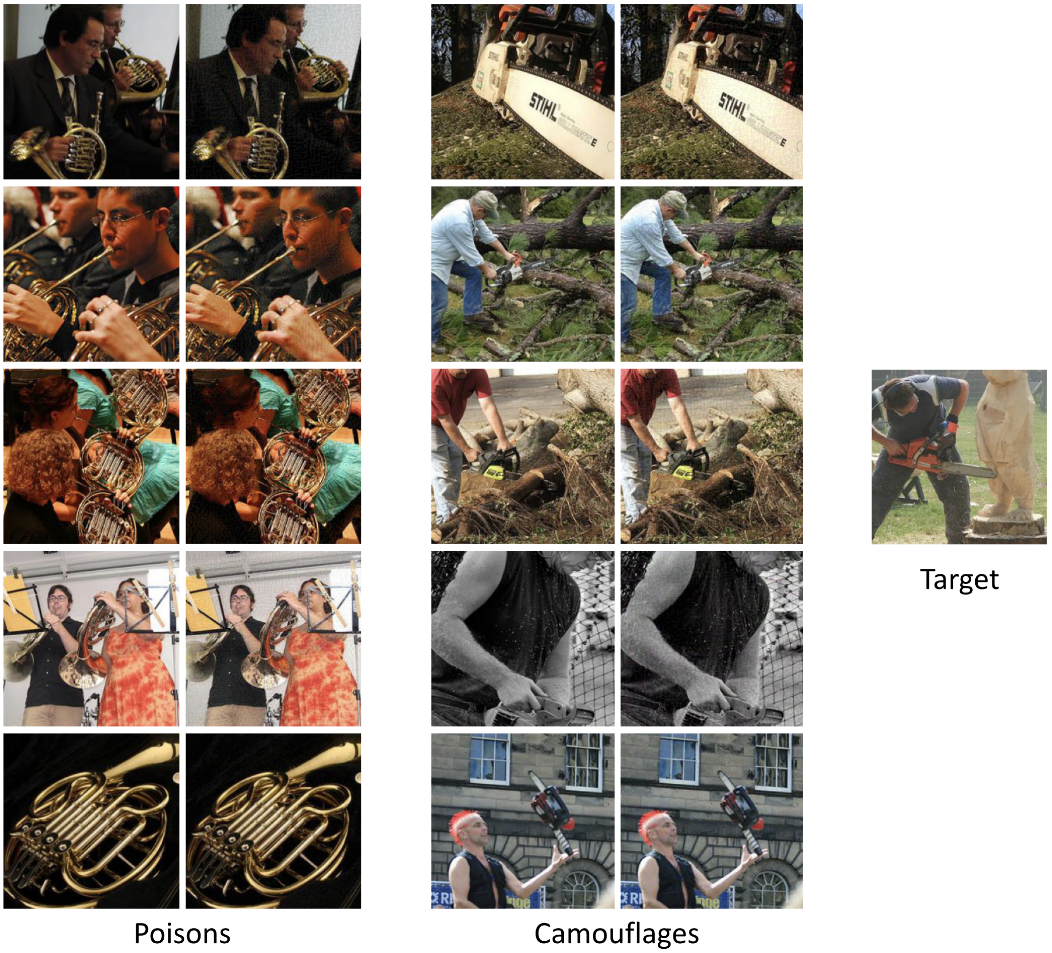

Figure 6: Visualization of poisons and camouflages on Imagenette dataset. The first and the third columns shows the original images, and the second and the fourth columns shows the corrupted images (with added Δ). The shown images were generated for a camouflaged poisoning attack on ResNet-18, with Seed = 2000011111 and ε = 8. The target and camouflage class is *chain saw*, and the poison class is *French horn*.

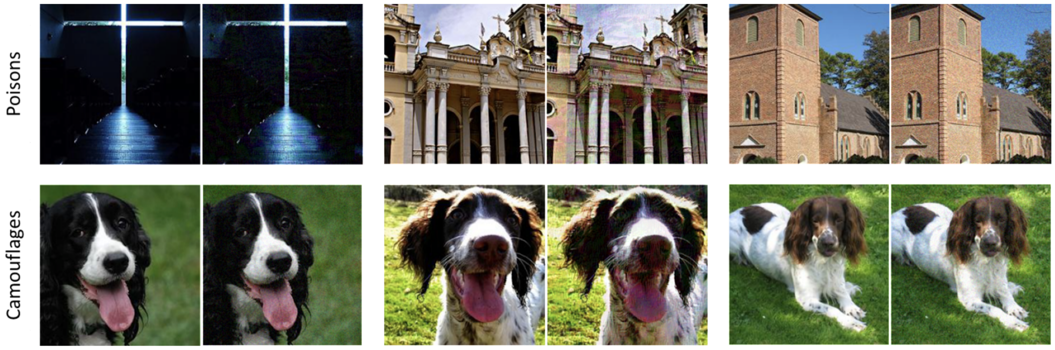

Figure 7: Some representative poison and camouflage images for attack on Imagewoof dataset. In each pair, the left figure is the original picture from the training dataset and the right figure has been adversarially manipulated by adding Δ. The shown images were generated for a camouflaged poisoning attack on Resnet-18, with Seed = 10000005, b_p = b_c = 6.6% and ε = 16. The target and camouflage class is *English Springer*, and the poison class is *Building (Church)*.

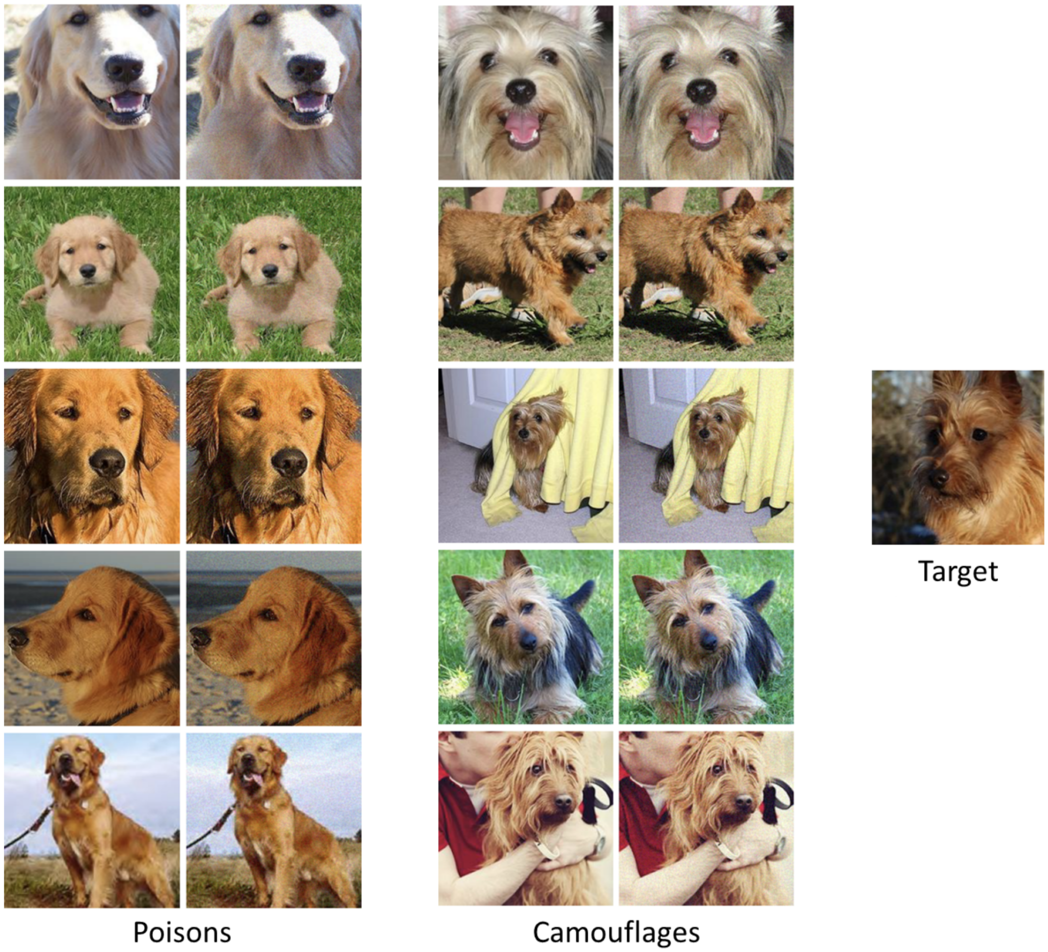

Poisons

Camouflages

Target

Figure 8: Visualization of poisons and camouflages on Imagewoof dataset. The first and the third columns shows the original images, and the second and the fourth columns shows the corrupted images (with added Δ). The shown images were generated for a camouflaged poisoning attack on ResNet-18, with Seed = 2111111110, b_p = b_c = 4.2%, ε = 16. The target and camouflage class is *Austrailian Terrier*, and the poison class is *Golden Retriever*.

B.6 Additional Experiments

B.6.1 Ablation study for different values of b_p and b_c

In this section, we explore the effect of changing the relative sizes of the poison samples and camouflage samples. The experiments are performed on ResNet-18 for CIFAR-10 dataset with $b_p = 1\%$ and $b_c = \{0.5, 1, 1.5\}\%$ respectively, and vice-versa. We report the results in Table 8.

One may also wonder what is the price that an attacker has to pay in terms of the success rate of a poisoning (only) attack if it chooses to devote a part of the budget for camouflages. In Table 9, we report the results for comparing the success rate 1% poisons and 1% camouflages, to success rate with 2% poisons (and no camouflages.)

Problem parameters		**Attack success**		**Validation Accuracy**		
b_p	b_c	Poisoning	Camouflaging	Clean	Poisoned	Camouflaged
1%	1.5%	83%	80%	0.822	0.8191	0.8264
1%	0.5%	83%	40%	0.845	0.8395	0.8432
1%	1%	83%	80%	0.822	0.8274	0.8244
0.5%	1%	33%	50%	0.822	0.8261	0.8194
1.5%	1%	83%	20%	0.822	0.8156	0.8118

Table 8: Effect of different sizes of poison and camouflage datasets on the success of the proposed camouflaged poisoning attack on CIFAR-10 dataset trained on ResNet-18, with $\varepsilon = 16$. The reported success rates are averaged over six different trials with seeds 200000111-211111111. For each experiment, we do 4 restarts for every poison and camouflage generation.

Problem parameters		**Attack success**		**Validation Accuracy**		
b_p	b_c	Poisoning	Camouflaging	Clean	Poisoned	Camouflaged
1%	1%	83%	80%	0.822	0.8274	0.8244
2%	0	83%	N/A	0.822	0.817	N/A

Table 9: Comparison of success rate when the allocated budget of 2% is split as: (a) 1% poisons and 1% camouflage, and (b) 2% poison samples and 0% camouflages. The experiment is performed on CIFAR-10 dataset trained on ResNet-18 with $\varepsilon = 16$. The reported success rates are averaged over six different trials with seeds 200000111 - 211111111. For each experiment, we do 4 restarts per poison or camouflage generation.

B.6.2 Robustness of our attack to random deletions

We next explore the effect of random removal of the generated poison and camouflage samples on the success of our attack. In a data-scraping scenario, a victim may not scrape all the data points modified by an attacker. In Table 10, we report the result where different amounts of the generated poison and camouflage samples are deleted uniformly at random.

Amount removed		**Attack success**		**Validation Accuracy**		
Poisons	Camouflages	Poisoning	Camouflaging	Clean	Poisoned	Camouflaged
5%	5%	80%	75%	0.822	0.823	0.819
10%	10%	60%	33%	0.822	0.817	0.825
20%	20%	80%	100%	0.822	0.826	0.820
30%	30%	100%	80%	0.822	0.8215	0.818
40%	40%	20%	100%	0.822	0.825	0.817

Table 10: Effect of random removal of the generated poison and camouflage samples on the success of the proposed camouflaged poisoning attack on CIFAR-10 dataset trained on ResNet-18, with $\varepsilon = 16$. The reported success rates are averaged over 5 different trials with seeds 200001111 - 211111111. For each experiment, we do 4 restarts for every poison and camouflage generation.

B.6.3 Transfer experiments

In this section, we show that the poison and camouflage samples generated by the proposed approach transfer across models. Thus, an attacker can successfully execute the camouflaged poisoning attack, even if the victim trains a different model than the one on which the poison and camouflage samples were generated. We show the transfer success in Figure 9. The brewing network denotes the network architecture on which poison and camouflage samples were generated (we adopt the same notation as Geiping et al. (2021)). The victim network denotes the model architecture used by the victim for training on the manipulated dataset.

We ran a total of 3 experiments per (brewing model, victim model) pair using the seeds 2000000000-2000000011. Each reported number denotes the fraction of times when both poisoning and camouflaging were successful in the transfer experiment, and thus the attack could take place.

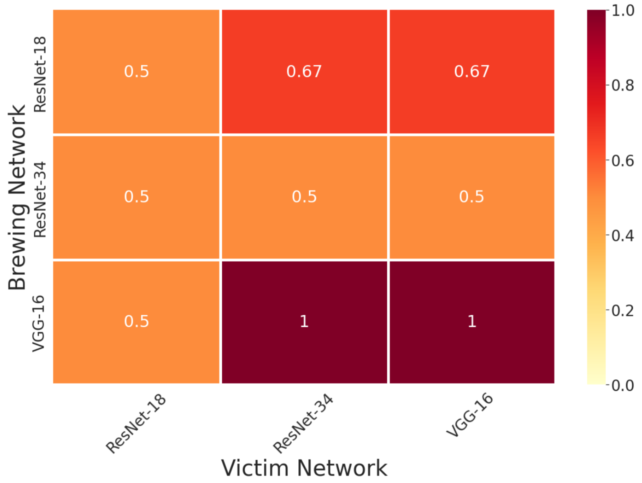

Figure 9: Transfer experiments on CIFAR-10 dataset.

B.6.4 Robustness to Data Augmentation

Data augmentation is commonly used to avoid overfitting in deep neural networks. In order to be applicable in the real life, our poisoning and camouflaging attacks must be successful even when the model is trained with data augmentation. In order to validate this, we evaluate our approach on CIFAR-10 dataset trained with data augmentation on ResNet-18 in the threat model $\varepsilon = 16, b_p = b_c = 1\%$; the results are in Table 11. The considered data augmentations are:

1. *No Augmentation*: Exact images from the training dataset are used.

2. *Augmentation Set 1*: 50% chance that the image will be horizontally flipped, but no rotations.
3. *Augmentation Set 2*: 50% chance that the image will be horizontally flipped, and random rotations in $\text{Uniform}(-10, 10)$ degrees.

The reported results in Table 11 are an average over 5 random seeds from ”kkkkkk” where $1 \leq k \leq 5$. As expected, the validation accuracy for the model trained on clean dataset increased from 82% percent when trained without augmentation, to 86% for augmentation Set 1 and 88% for augmentation set 2. The addition of data augmentation during training and re-training stages make it harder for poisoning to succeed and at the same time makes it easier for camouflaging to succeed.

Data Augmentation	**Attack success**		**Validation Accuracy**		
	Poisoning	Camouflaging	Clean	Poisoned	Camouflaged
No Augmentation	100%	20%	82%	82%	82%
Augmentation Set 1	86%	33%	86%	85%	86%
Augmentation Set 2	60%	100%	88%	86	86%

Table 11: Effect of data augmentation on our proposed camouflaged poisoning attack.

B.6.5 Similarity of the feature space distance

A natural approach to defend against dataset manipulation attacks is to try to identify the modified images, and then remove them from the training dataset (i.e., *data sanitization*). For instance, one could cluster images based on their distance from their class mean image, or from the target image. This type of defense could potentially thwart watermarking poisoning attacks such as Poison Frogs (Shafahi et al., 2018). As we show in Figure 10, such a defense would not be effective against our proposed poison and camouflage generation procedures, as the data distribution for the poison set and the camouflage set is similar to that of the clean images from the respective classes.

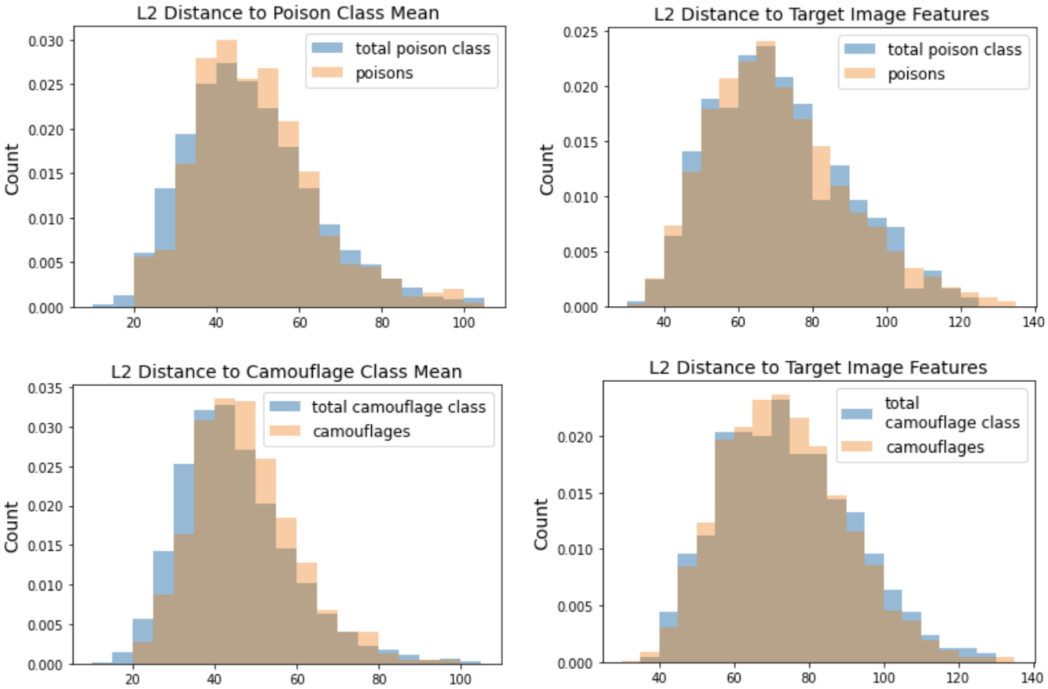

Figure 10: Feature space distance for our generated poison and camouflage set. The reported data was collected by a successful camouflaged poisoning attack on Resnet-18 model trailed on CIFAR-10 with seed 2000000000, ε = 16 and b_p = b_c = 1%.